Linköping University |Department of Physics, Chemistry and Biology
Master of Science Thesis, 30 ETCS | Applied Physics
Spring 2018 | LITH-IFM-A-EX—18/3573—SE

In Situ Heating During XRD Measurements as a Method to Study Recrystallisation of Aluminium Alloy AA3003

Louise Bäckström

Supervisors: **Lars-Åke Näslund**, Gränges R&I
Fredrik Eriksson, IFM, Linköping University

Examiner: **Per Eklund**, IFM, Linköping University

LINKÖPINGS UNIVERSITET

Upphovsrätt

Copyright

Abstract

Recrystallisation is an important topic in the metal industry since the process may drastically alter the properties of the materials subjected to it. By controlling the recrystallisation process, the material properties can be adjusted as desired, which could lead to stronger materials and hence lighter constructions, decreasing our material consumption. This is currently regulated using softening curves complied from tensile tests, a method which does not show the degree of recrystallisation of a metal. This thesis work therefore explores the possibility to characterise the recrystallisation process using *in situ* X-ray diffraction, XRD, during heating.

The method proposed is using *in situ* heat treatments of aluminium samples combined with XRD measurements. The results show that it is possible to follow the recrystallisation process of rolled aluminium alloy AA3003 by using *in situ* XRD during heating, a discovery that could facilitate development and understanding of new materials. Nevertheless, further investigations of the subject is required before the method will be profitable.

Sammanfattning

Rekristallisation är ett viktigt ämne inom metallindustrin, detta eftersom materialegenskaper drastiskt kan förändras under rekristallisationsprocessen. Genom att kontrollera rekristallisationsprocessen kan materialegenskaper skräddarsys efter applikation. Även starkare material kan tillverkas och därav kan lättare strukturer konstrueras och på så vis minskar även materialåtgången. Idag regleras rekristallisation med hjälp av mjukningskurvor sammanställda genom dragprov, en metod som inte kan visa rekristallisationsgraden av en metall. Detta examensarbete utforskar möjligheten att karaktärisera rekristallisationsprocessen genom att använda *in situ* röntgendiffraktion, XRD, under värmningsprocessen.

Den framtagna metoden inkluderar *in situ* värmebehandlingar av aluminiumprover i kombination med XRD-mätningar. De erhållna resultaten från experimenten visar på att det är fullt möjligt att följa rekristallisationsprocessen av aluminiumlegering AA3003 med *in situ* XRD, en upptäckt som kan komma att underlätta vid utveckling och förståelse av legeringar och nya material. Dock krävs fortsatta studier i ämnet innan metoden kan anses vara lönsam.

Acknowledgement

This master thesis is for fulfilment of the degree master of science in biomedical engineering, with master in applied physics at Linköping University. The thesis is of 30 credits, and has been conducted in association with Gränges Sweden AB in Finspång. First and foremost, I would like to express my sincere gratitude towards Gränges for the opportunity to perform my thesis work for the company and for welcoming me into Gränges R&I. Further I am grateful to all employees at Gränges R&I who made this thesis possible and who helped during the project. Finally, I would like to thank my family and friends for encouragement and moral support. Without all of you, the outcome of the thesis would not have been the same.

Special thanks to:

Lars-Åke Näslund, *supervisor at Gränges*, for implementation of the project, as well as guidance and help throughout the entire work.

Fredrik Eriksson, *supervisor at IFM*, for education in operating the diffractometers and patiently helping during experiments.

Per Eklund, *examiner*, for helping in setting up the thesis at Gränges and answering questions.

Evelina Hansson and **Birger Bäckström**, for reading and providing feedback on this report.

Emil Åhlin, for proofreading, feedback and support.

Linköping, June 2018
Louise Bäckström

Table of Contents

List of Figures

List of Tables

List of Abbreviations and Acronyms

AA	Aluminum Association
DC	Direct Chill
EBSD	Electron Back Scatter Diffraction
EN AW	European Norm Aluminium Wrought
LOM	Light Optical Microscope
SEM	Scanning Electron Microscope
TEM	Transmission Electron Microscope
XRD	X-ray Diffraction

1 Introduction

When a polycrystalline metal is heated to a, for the material, specific temperature the grains of the metal will undergo recrystallisation. During this process the mechanical properties of the material may drastically change. During this thesis work, conducted at Gränges R&I in Finspång and IFM at Linköping University, the changes in grain structure are to be characterised utilising X-ray diffraction, XRD. Below follows an introduction to the project incorporated in this thesis, starting with the purpose and goal of the work.

1.1 Purpose of Thesis

Rolled aluminium often attains a fibrous structure, making the material hard, and is therefore difficult to shape to desired form. With heat treatments, it is possible to obtain a softer, more ductile material. This change in material properties is because of recrystallisation, and at a complete recrystallisation the ductility of the material is at its peak. As the degree of recrystallisation of the material changes, so do the material properties. The material properties, as an effect of recrystallisation, are currently regulated using softening curves, a method which is not accurate in estimating degree of recrystallisation.

If degree of recrystallisation can be determined using *in situ* heat treatment during XRD measurements, this would open up for further investigations in the field. A fully developed method of this kind could, in the long run, save both time and money for companies developing and testing metals or alloys for specific areas of use.

1.2 Goal

The goal of this thesis is to characterise the recrystallisation process using XRD in combination with a heat treatment of the material. Included is the development of the characterisation method, independent XRD measurements, both standard and using *in situ* heating, and analysis of received data.

1.3 Background

This thesis work will be performed at the company Gränges Sweden AB, specifically on the department of research and innovation, Gränges R&I, in Finspång, Sweden. The results and conclusions drawn from this work may be utilised by Gränges during further studies in the field.

1.3.1 Gränges Sweden AB

Gränges Sweden AB was founded in 1896 in the Swedish town Grängesberg where multiple local industries were included in the group. In 1922 the company started their production in Finspång, where it still remains today. Later, in 1969, Gränges acquired Svenska

Metallverken, and a few years later, in 1972, the company was developed into Gränges and Sapa. The company now began their production and development of aluminium for heat exchangers in Finspång. In the beginning Gränges worked with several different metals, however since Electrolux acquired the company in 1980, only the production of aluminium remains. Over the years Gränges has expanded their operation abroad, the company established production in Shanghai 1996 and acquired the American company Noranda in 2016, Noranda later changed name to Gränges Americas Inc. In 2005 Gränges was acquired by the Norwegian company Orkla, however since 2013 Gränges is once again a self-sufficing company and in 2014 the company was listed on the Nasdaq Stockholm Stock Exchange. [1]

Today, Gränges have approximately 1600 employees worldwide and the head office is situated in Stockholm. The total production capacity of the company is currently 420 000 tonnes, slightly above the sold amount of material at 336 000 tonnes. The average total sales per year can be summarised to approximately 10.15 billion SEK. [2] Further, the company has production sites worldwide, with locations in Finspång, Shanghai, Huntingdon, Salisbury and Newport. [3]

Gränges is almost exclusively focusing on producing rolled aluminium for manufacturing of heat exchangers and is one of the largest in the industry with their products. The heat exchangers manufactured are constructed from several different materials, which are using different alloys depending on function and requests from customers. [2]

1.3.2 Aluminium

Aluminium is the most common metal in the crust of the earth and has been frequently used since the beginning of the 20th century. Although the metal has been used for over 6000 years, it was not until the early 19th century that pure aluminium was first extracted, using an extremely inefficient method. The revolution for the aluminium industry came in the late 19th century when the Bayer-process and the Hall-Héroult method were developed. These processes for extraction and fabrication of the metal are still used today. During the last 50 years the industrial use of aluminium has increased exponentially and today the metal is one of the most used in society, with applications in almost every field of industry. [4]

The exponential increase in aluminium usage is because the metal is light and easily machined, while simultaneously strong and corrosion resistant. Furthermore, the material is quite conductive and easily modified to be applicative in any area of use. Aluminium is often alloyed with other metals in order to further modify the material properties, and so, extend the industrial applications. Today the metal is used for numerous applications, among many others, auto and construction industries and in the biomedical industry to manufacture tools and medical appliances. [4]

1.3.2.1 Properties

Aluminium has the atomic number 13, chemical designation Al and a lattice constant of 4.05 Å [5]. The melting temperature of the metal is 660 ^{o}C. Since the break of the 20th century

aluminium has gained popularity within industry. This because aluminium is a light metal, with a density of 2698 kg/m^3, which is close to a third of the weight of stainless steel. This property of aluminium makes it possible to build lighter constructions, which is desirable in for example the auto and construction industries. Apart from being light, aluminium also have good electrical and thermal conductivity, approximately 60 % of the conductivity of copper. [6]

Aluminium itself has good resistance to corrosion, owing to its protective oxide layer that naturally forms on aluminium surfaces. Although this corrosion resistant oxide layer is only effective in a specific pH interval. To change this interval the material can be alloyed or otherwise treated, to obtain appropriate corrosion resistivity. Furthermore, aluminium is both easy to use and to shape, because of its ductility. The many options in moulding aluminium has further made aluminium a popular choice as a construction material. [4] [6]

Aluminium is highly recyclable and the energy needed to extract aluminium from recycled materials is only 5 % of the energy needed for the process described in section 1.3.2.2 below. Hence it is very attractive for producers to recycle aluminium from used products.

1.3.2.2 Production

Aluminium rarely exist naturally in some other form than its oxides and hydroxides. Therefore bauxite, an aluminium ore composed of different aluminium hydroxides, is mined and refined to obtain the pure aluminium.

The first step of the process is to extract aluminium oxide from bauxite. This is normally done according to the Bayer method, which basically states that aluminium hydroxides are easily dissolved in lye, NaOH, and that the solubility is dependent on the temperature. During the process ground bauxite is mixed with NaOH at elevated temperature and high pressure, wherein a sodium aluminate, $NaAl(OH)_4$, solution is formed. As the temperature is lowered, $NaAl(OH)_4$ precipitates from the solution. The hydroxide is then both filtered and depurated, before heated to 1200 – 1300 ^oC. At this temperature the chemically bond crystal water is evaporated and aluminium oxide, Al_2O_3, is obtained. Throughout the years other methods have been developed to reduce the energy consumption and to extract aluminium from other aluminium ores than bauxite. [4]

Aluminium has a high affinity to oxygen, thus the extraction of pure aluminium from Al_2O_3 is conducted using igneous electrolysis according to the Hall-Héroult process. Since Al_2O_3 has a melting temperature of 2060 ^oC, the oxide is diluted to approximately 5 % in cryolite, Na_3AlF_6, and aluminium fluoride, AlF_3, to decrease the melting point to 960 – 980 ^oC. The current needed to melt the blend is 100-300 kA, and the voltages used is often 4 V. In order for the anode and cathode to withstand the harsh conditions they are constructed using almost exclusively coal. Due to the high currents used the process is energy consuming, and according to theoretical calculations 1 kAh will yield about 340 g aluminium, however the efficiency of the process is 95 % at best. The Hall-Héroult process has been used for over

100 years without any major changes. Only the efficiency of the process and manufacturing of anode and cathode has been renewed. [4]

Following the electrolysis is casting of the aluminium, this is usually done directly or semi-directly with DC casting or strip casting. Wherein the former, the molten aluminium is purified from remaining oxides and dissolved hydrogen before moulded into large ingots. The casting is water cooled and the moulds are controlled to keep the casting speed and the intensity of the cooling stable, in order to obtain a uniform structure of the material. With today's technology the water cooling can be replaced by an electromagnetic field, holding the metal in place until the surface is solidified. This is slightly more energy efficient and provides high quality surfaces of the ingots. During strip casting, the molten aluminium is directly transported to a rolling mill where the melt solidifies between the rollers. This form of casting can only be used for rolled products, however for these products the method provides a more energy efficient alternative since no hot rolling of the metal will be needed. During strip casting the cooling rate is much higher than during DC casting, which leads to smaller grains in the material. Therefore, the method is most suitable when manufacturing thin strips and foil. [4]

Next in the production process is, for rolled goods, hot and cold rolling. If strip casting was not performed the aluminium is hot rolled. During hot rolling the ingots are heated to 450 – 550 ^{o}C and are then rolled to a thickness of a few millimetres. Over the course of this process the temperature, reduction rate, and lubrication matters to properties like grain size, surface quality, and texture of the rolled aluminium. During cold rolling no heating of the material is performed, the process rather utilises the ductility of aluminium to deform the metal. Now the already rolled material is further thinned to a desired thickness, sometimes as thin as 5 µm. Instead of rolling the aluminium the material can be wrought in several different ways, extrusion or forging, among others. [4]

1.3.2.3 Alloying and Other Treatments

In order to modify the properties of the material, aluminium is often alloyed with other substances. Usually the alloying element is added to the aluminium right before DC or strip casting is performed. [4]

All aluminium goods belong to one of eight alloy series, where within one series the alloys show similar characteristics in terms of mechanical properties, corrosion resistance, and castability. Common alloying elements used to form aluminium alloys are copper, manganese, silicon, magnesium, and zinc, which all determine the basic properties within the same series. The designation of the different aluminium alloys is usually named accordingly with AA, or in Europe EN AW, where each alloy is denoted by a four-digit number. The first digit indicate the main alloying element, according to Table 1.1. The second digit of series 2 – 9 indicate if modifications to the alloy have been done, where zero means that no changes have been made. So called additives may be added to the alloy, these are elements such as copper or magnesium. They rarely make up more than one percent of the total alloy, but an alloy can

contain several different additives, to increase certain properties. Therefore, the two last digits are used to identify the individual alloys in the series. [6] [7]

Table 1.1: Corresponding series for main alloying metals.

Series	Alloying Element
1 XXX	Pure aluminium, no alloying metal
2 XXX	Copper, Cu
3 XXX	Manganese, Mn
4 XXX	Silicon, Si
5 XXX	Magnesium, Mg
6 XXX	Magnesium/Silicon, Mg/Si
7 XXX	Zinc, Zn
8 XXX	Blend
9 XXX	For future use

Aluminium alloys can be separated into two groups: age-hardenable and strain-hardenable alloys. Age hardening is performed by first heating the alloy to a specific temperature, after which the metal is quenched to obtain a solid solution. The material is then naturally aged, in room temperature, or artificially aged, at elevated temperatures, approximately 100 – 200 ^{o}C. [6]

During strain hardening plastic deformation from rolling, stretching, and bending causes changes in grain structure of a material. Strain hardened alloys are usually marked with a temper to show how the material has been treated or deformed. The three used designations are F, O and H, which denote material that has been through no deformation, annealing, and strain hardening, respectively. The latter can be assigned a two digit number to further specify the properties of the material. The first digit, 1, 2, or 3, show if the alloy has been strain hardened, strain hardened and partially annealed, or strain hardened and stabilised by heat treatments. The second digit, 1 – 9, indicates the hardness of the metal, where 8 is fully hard corresponding to 75 % reduction, 4 is half hard equivalent to 25 % reduction, etc. The number 9 denotes extra hard materials, this because the degree of hardness originally was defined from the measured strength of pure aluminium. For some alloys it is therefore possible to obtain a harder material than fully hardened pure aluminium. [6] [7]

The metal can be either homogenised or unhomogenised, meaning that the grains in the material are small and evenly distributed or large, respectively. Homogenisation of a material is performed after casting is complete, at temperatures below the melting point, for aluminium usually between 500 – 600 ^{o}C. At these temperatures the recrystallisation process is fairly slow due to the recrystallisation front being controlled by migrating high-angle boundaries. [8] This allows diffusion of interstitials and additives in the solid solution, which evens out the unevenly distributed concentrations throughout the ingot. To simplify the initiation of the recrystallisation process, impurities of some kind can be added to the alloy to create crystalline starter points. An unhomogenised metal is not annealed after casting and may

therefore hold differences in concentration throughout the casted ingot. Further the grain growth of crystals may appear irregular and thus the grain sizes will vary in an unhomogenised metal. [4] [9]

1.3.2.4 AA3003

Aluminium alloy AA3003 is a very common alloy and is a member of the 3000 series and has therefore manganese, Mn, as its main alloying element. The alloy is a strain hardenable alloy. Adding manganese to aluminium enhances the materials resistance to corrosion, improves mechanical properties, and facilitates deep drawing of the metal. Manganese in solid solution with aluminium increases the strength of the material more than if precipitates of manganese are formed in the alloy, *vice versa* for the ductility. Since the formation of precipitates occur at lower temperatures, or slower cooling, the mechanical properties are highly dependent on the cooling rate of the alloy. [6]

Table 1.2: List of elements and amounts allowed in AA3003. [10]

Element	Amount [%]
Aluminium (Al)	96.8 – 99.0
Manganese (Mn)	1.10 – 1.50
Copper (Cu)	0.05 – 0.20
Iron (Fe)	0.00 – 0.70
Magnesium (Mg)	0.00 – 0.05
Silicon (Si)	0.00 – 0.6
Zinc (Zn)	0.00 – 0.10
Residuals (Total)	0.00 – 0.15
Residuals (Each)	0.00 – 0.05

AA3003 has a slightly higher density, 2730 kg/m^3, than pure aluminium caused by it containing heavier elements. The alloy's melting temperature, 643 – 654 ^{o}C, is lower than that of pure aluminium, 660 ^{o}C. Areas of use for AA3003 are sheet-metal fabrication, vehicle industries, buildings and heat exchangers, due to its diversity of properties. [6]

1.3.3 Recrystallisation

After deformation of a crystalline material the free energy is raised because of the appearance of dislocations. This will change certain properties, such as ductility and strength, since the higher energy will induce thermodynamic instability to the material. In order to restore the internal energy, crystallite structure and size changes, a process which is called recrystallisation. Recrystallisation can also be induced or hastened by annealing, or brazing, the material. [8]

1.3.3.1 Stored Energy in Materials

Grain boundaries in a material often hold some dislocations since grains generally grow in different directions. Therefore there will be a certain angle between the crystal planes of the different grains. At low-angle grain boundaries, with a maximum angular difference of

10 – 15º, the grain boundary energy is almost linearly dependent on the angle. This is because of the increasing strain in the material for the crystal planes to fit into each other. At higher angles the energy levels off since the effects of strain and formation of dislocations may counteract. [11]

1.3.3.2 Deformation of Materials

When a material is deformed, for example cold rolled, the microstructure is altered. The most obvious change in this case is that the grains change shape, which lead to an increase in the total grain boundary area. Thus, more strain and dislocations are present in the material and the stored energy will therefore increase accordingly. Further, when deformed, an internal structure of the grains may appear because of the accumulation of dislocations due to interstitials or vacancies in the material. [8]

During deformation of a polycrystalline material the individual grains might change orientation in relation to the applied stress. Hence, these changes are not random and acquire a preferred orientation of the material, called texture. The texture becomes more palpable with larger deformation or reduction rate. [8]

1.3.3.3 Recovery

Since a deformed material is thermodynamically unstable, the defects may spontaneously disappear. This is called recovery and is a slow process, especially at low temperatures, driven by the elastic energy stored in dislocations. During recovery the microstructure and some parts of the original properties might be restored as a result of the disappearance and rearrangement of dislocations. The process occurs relatively homogenously throughout the metal and does not usually affect the grain boundaries of the deformed grains, but subgrains are formed. In cold rolled Al-Mn alloys recovery of the metal usually takes place during heating to 200 – 250 ºC. The forces restraining growth of the subgrains are mainly surface energy of the grain boundaries. [8] [12]

1.3.3.4 Recrystallisation

Since the dislocations are usually present in the material even after recovery, the material still has elevated levels of free energy, although after recovery it reaches a metastable state. In order to further restore the material additional energy is supplied to the metal, usually through heat, to initiate and accelerate the process. With the extra energy, new grains, free of dislocations, are formed in the material, a process referred to as recrystallisation. Recrystallisation is most easily induced in remaining grain boundaries or impurities, since these hold a larger free energy. The temperature at which the process takes place is generally approximately 60 % of the melting temperature of a given metal. [8] [11]

Most commercial materials contain at least two phases, this also applies to AA3003. The dispersed particles can be present in the material during deformation or precipitate during annealing processes through production. In AA3003 manganese will, when heated, form precipitates with aluminium, resulting in grains of Al_6Mn which are mainly situated in the grain boundaries of the solid solution. Depending on when the precipitates are formed their

presence in the material will affect the recrystallisation process differently. There are three possible cases, precipitation before, during, or after recrystallisation. [8]

If precipitation occurs before recrystallisation, the presence of closely spaced dispersoids may inhibit the recrystallisation process due to pinning effects on the grain boundaries. However, if the particles are large, the dispersoids may act as nucleation sites for possible recrystallisation. Larger precipitates can also be obtained through particle coarsening, although this process would be extremely slow in AA3003 since the recrystallisation temperature of the alloy is rather low. By adjusting the heating rate it is possible to shift the recrystallisation temperature, sometimes as much as 100 ^{o}C. Generally a slower heating rate will result in an increased recrystallisation temperature and *vice versa*, although this can vary significantly depending on the alloy. [8] [12]

For precipitation during recrystallisation the recrystallisation process actually starts slightly before precipitation, but subsequent precipitation will impede the recrystallisation to be completed. The amount of recrystallisation that occur is strongly dependent on the annealing temperature, where a higher temperature will yield a higher degree of recrystallisation. [8]

If no significant precipitation occurs until recrystallisation is completed, there will be little to no effect on the process and it will proceed as if in a single phase alloy. The grains grown are more often equiaxial in structure and smaller than the grains formed if precipitation occur before or during recrystallisation. However, a significant grain growth can be seen in these materials. [8]

1.3.3.5 Grain Growth

After recrystallisation dislocations are removed, however the material will still contain grain boundaries, which are thermodynamically unstable. Therefore, if more energy is added the larger grains will grow at the expense of the smaller, so called Ostwald ripening. This process is called grain growth and occurs since it is more energetically favourable for a crystal to have a large volume to area ratio. The larger the grains the less grain boundaries will be present in the material, thus the lower the energy. [8] [13]

The main influencing factors affecting grain growth are temperature, solutes, sample size, and texture. Since grain growth mainly is migration of high-angle grain boundaries the energy consumption of the process is high even though the driving force for grain growth in a material is relatively low. Hence, grain growth are almost exclusively found at very high temperatures. Both solutes and other particles in the sample will inhibit grain growth. This since the solutes often are situated in or close to the grain boundaries, thus mechanically hindering the grain growth process. The limit of grain size in a material may therefore be related to the distance between interparticles. If the thickness of the sample is smaller than the existent grains, high-angle boundaries will only exist in 2D, rather than 3D. This will consequently inhibit grain growth since the driving force of the process is reduced significantly. Texture can too impede grain growth, because a strongly textured material contain mainly low-angle grain boundaries. [8] [12]

1.4 Related Work

No publication of identical work was found, however similar studies have been conducted on both cold rolled copper [14] and cold rolled gold [15]. Further, Poulsen et al. [16] are using 3D XRD to study growth kinetics of individual grains during recrystallisation in aluminium. Even different experiments have been conducted calculating grain size and distribution [17] as well as recrystallisation during *in situ* heating [18]. In all cases XRD, of some kind, is used to investigate some aspect of the recrystallisation process, however, other characterisation methods, SEM, TEM, or EBSD, have been utilised to confirm and complete the results.

1.5 Limitations

During this work, only one aluminium alloy, the common AA3003, will be examined. However, to obtain a complete perception of the material and its properties, both homogenised and unhomogenised metal will be analysed. Further, the four different production tempers, which are H18, H14, H24, and O, described in sections 1.3.2.3 and 3.1, will be examined using regular XRD measurements. *In situ* heating will only be performed on H18, for both homogenised and unhomogenised material.

In the scope of the thesis, the focus will be on characterising the recrystallisation process using XRD and therefore no other technique, apart from LOM, will be used to substantiate the data obtained.

1.6 Problem Statement

From the purpose of the thesis stated above, the problem statements can be more specifically presented as the following questions.

- Is it possible to characterise the recrystallisation process in aluminium alloy AA3003 using *in situ* heating during XRD?

- Can the method be used as a complement to the traditional softening curve?

1.7 Report Structure

This report is constructed to be easy to follow for the reader, starting with an introduction of the project, with the aim and purpose of the thesis work, and a background covering relevant information about the work. Following is a section containing the theory needed to comprehend the basics of the study and experiments performed, later followed by the methodology used. The report then proceed with a presentation of the obtained results. Continuing with analysis and discussion of said results and finally conclusions drawn from the results.

In this report the referring system will follow the standards of the Vancouver method. References situated at the end of a paragraph are referring to the entire section. However, when situated within a sentence, it only refer to the information stated in said sentence. The references are then listed, in the order they appear in the report, in the list of figures. All figures and tables taken from external sources will be referred to using the same standard method, hence figures and tables lacking references are made by the author.

2 Theory

The following chapter is comprised of relevant theory regarding the work conducted. The purpose of the written theory is for the reader to gain sufficient knowledge in the field to comprehend the experiments and analysis performed over the course of the thesis work.

2.1 X-Ray Diffraction

XRD is a non-destructive analytical technique which gives crystallographic information about a specimen. The technique studies the interaction of monochromatic X-rays and the periodic crystal lattice of a material. The penetration depth of X-rays varies depending on the energy and incidence angle of the X-rays and the electron density of the sample. Generally, X-rays will only penetrate the surface of the material, reaching a few µm into the material, and therefore only information about the crystal grains near the surface can be analysed. [19]

The method was first invented through a cooperation of Debye, Scherrer and Hull in 1917. Since this first diffractometer the technique has been refined and improved, and several features has been added. The most palpable change is the computer aided X-ray diffraction measurements, developed about 50 years after the invention of the method. Despite the improved techniques the working principle has remained the same over the course of the century, although, now more complex algorithms are utilised to identify different crystal structures of powders and solids. Today, XRD is widely used in various fields of scientific work and a must-have for many research teams. [20]

2.1.1 The instrument

An XRD instrument is relatively simple regarding its structure, basically only containing an X-ray source, a sample holder and a detector mounted on a goniometer. The X-ray source is pointed towards the sample placed in the sample holder. Usually the sample holder acts as a reference of the sample position. Both the detector and the X-ray source can be displaced to obtain different incident and diffraction angles onto the sample. To the detector a computer is connected, showing the results from the measurements. [19]

2.1.2 X-Ray Generation

X-rays can be generated in numerous ways. The most common, and applied in the used XRD equipment, is described below.

A tungsten filament is heated, using a current of approximately 40 mA, to the point where electrons are emitted from the filament by thermionic emission. The electrons are accelerated towards a metal target, usually a copper disk, using a potential of 40 kV. When the electrons strike the metal target on the focal spot, X-rays are emitted in all directions. These X-rays are extracted from the X-ray tube through a beryllium window. [19]

The radiation emitted can be divided into two different types, bremsstrahlung and characteristic radiation. The bremsstrahlung has a continuous spectrum because of the deceleration of the high energy electrons through their interaction with the target plate atoms. The characteristic X-ray radiation, on the other hand, has a well-defined energy and arises as a result of electronic transitions when exited electrons fall back to the core level. The characteristic radiation may further be divided into different peaks, e.g. K_α and K_β, where K_α has the higher brilliance and is therefore the one used. An illustration of a common X-ray spectra can be seen in Figure 2.1. [21] In order to filter out the energies from the bremsstrahlung and K_β a filter is used. For a copper anode this filter is a nickel foil since it has a high absorption for copper K_β and preserves most intensity of the copper K_α peak. [22]

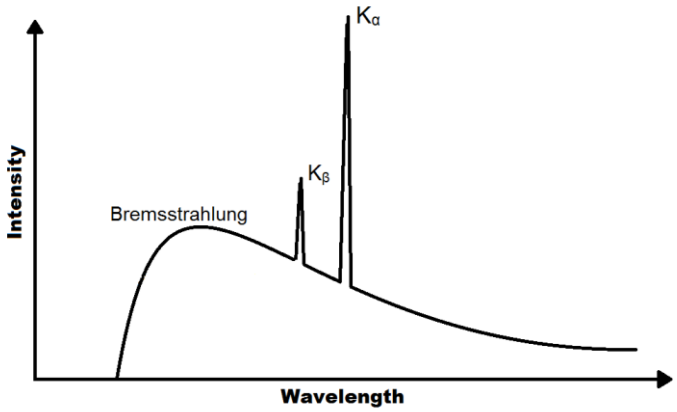

Figure 2.1: Continuous and characteristic X-ray spectra.

2.1.3 Working Principle

X-rays extracted from the X-ray tube are directed towards the sample. When the X-ray photons hit the sample the photons react with the material in several different ways, however in XRD only the diffracted photons are of interest. [19]

During diffraction the X-rays are scattered on the different crystal planes in the sample material. Constructive interference between two of the scattered beams can occur if they are in phase. This will exclusively occur if the incidence angle and the scattering angle are equal. Thus, diffraction only occurs for distinct angles depending on the interplanar spacing. This phenomenon can be expressed using Bragg's law, seen in Equation 1 below. [19]

$$2dsin\theta = n\lambda \qquad \text{Eq. 1}$$

Where d is the interplanar spacing, θ is the incident and scattering angle, λ is the wavelength of the X-rays used, and n is an integer. [19]

2.1.4 Analysis

In order to characterise peaks in the diffractogram, the lattice constants, found in tables or software, of the correspondent peak positions are calculated using Bragg's law. For cubic lattices, which are expected in this case, the interplanar spacing, d, is dependent on the lattice constant, a, and the Miller indices according to Equation 2. [19]

$$d_{hkl} = \frac{a}{\sqrt{h^2+k^2+l^2}} \quad \text{Eq. 2}$$

By combining Equation 1 and Equation 2 it is possible to calculate the lattice constant through Equation 3 below.

$$a = \frac{\lambda}{\sin\theta}\sqrt{h^2+k^2+l^2} \quad \text{Eq. 3}$$

The intensity of the peaks in an acquired diffractogram can depend on several different factors, for example the atomic form factor and structure factor [19]. When using powdered samples the diffractograms of samples with the same composition will always look more or less identical since the distribution of grains in a fine powder is random. When using non-powdered polycrystalline materials this is not always the case. This since texture matters to both the crystallite size and orientation of individual grains. The intensity is measured in counts, or counts per second, and is dependent on the amount of reflected radiation at a specific angle. Therefore, an increase in a peak's intensity may be caused by mass and areal gain of grains with the same orientation within the illuminated volume. Thus, the change in peak intensity can be seen from sample to sample. By calculating the area beneath the peak curve of the diffractogram, it should be possible to estimate grain size and distribution in the illuminated volume. [16] [17]

In the obtained diffractogram the peaks might appear thin or broadened. If broadened, this generally depends on two major causes, which are strain in the material or a small crystallite size. Even the environment in the diffractometer can have an impact on said broadening. If the instrumental broadening is extracted, the micro strain and crystallite size can be calculated based on the intrinsic broadening of the material, when comparing the diffractogram to that of a perfect single crystal. [17]

Since the X-rays produced generally contain both K_α and K_β radiation this can sometimes be seen as double peaks in the diffractogram. This is common especially for materials containing high quantities of silicon because silicon generates unusually high intensity peaks. However, the double peaks can usually be removed by using an additional Ni-filter, to further filter out the undesirable wavelengths. Since not much silicon is expected in the samples this is not considered a problem, and an additional filter should not be necessary. [23]

2.2 Light Optical Microscope

The first LOM was constructed in 1595 and the technique has developed a great deal since, however the principle remains the same. The technique utilizes visible light and optical lenses to view and magnify images of a chosen specimen. By illuminating the specimen with parallel rays of light, which has passed through several different optical lenses, a modern microscope can give magnifications up to 1200x. [22]

Today there are many different kinds of LOM, developed for a wide range of applications. Two of the most common are the transmission microscope and the reflection microscope. In a transmission microscope the light passes through the specimen to later reach the eye. In the reflection microscope the light is instead reflected onto the sample. This method is commonly used in metallographic studies, since metals are not transparent and therefore transmission microscopy is not an option when using visible light. With a reflection light microscope, a so called metal microscope, the surface of the specimen can be examined. [22]

By oxidising samples, especially done when working with aluminium, the oxide layer will grow on top of the surface grains of the sample. This results in individual grains with different orientation on the surface which are visible in reflection LOM since the light is diffracted differently on the oxide grains. [12]

2.3 Heat Treatment

During the production the material is subjected to different treatments to obtain the four tempers used, as described in 1.3.2.3. Since the four tempers have been subjected to dissimilar series of deformation and annealing, a difference in grain structure is expected. Further a difference in crystallite size is expected when comparing homogenised and unhomogenised materials. [8] [9]

As can be seen in Figure 2.2 a clear difference between the tempers can be distinguished. Fibrous structures are visible for H18 and H24, while H14 and O show a more granular structure. The tensile strength of H24 and H14 are per definition the same, but a significant difference in grain structure is noted. This since H24 is partially annealed the material is recovered, softening it, while in H14 fully annealed grains appear elongated due to partial deformation. Furthermore, the crystallite size obtained in the unhomogenised metal, to the right in the figure, is significantly larger than the grain sizes seen in the homogenised samples.

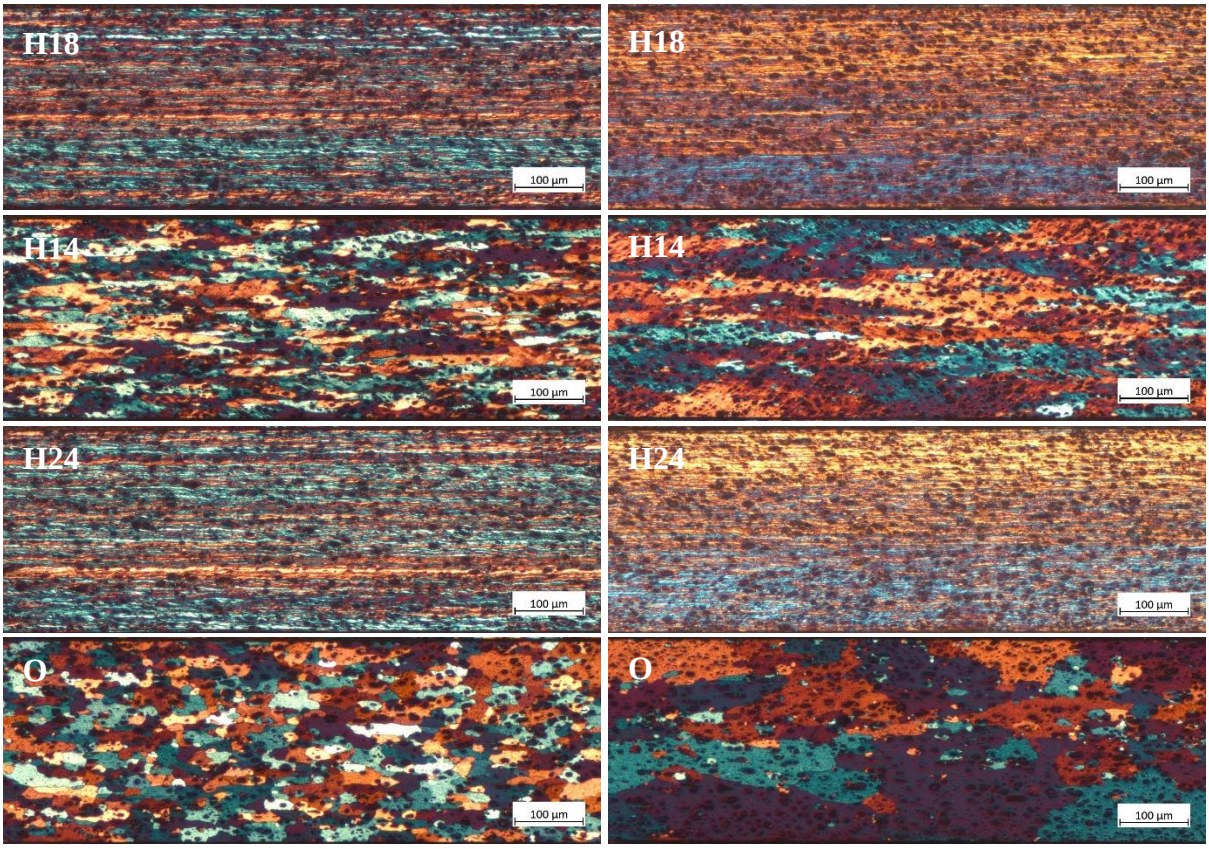

Figure 2.2: LOM images of AA3003 at different tempers, homogenized to the left and unhomogenized to the right.

As described in section 2.1.4 above, the intensity of peaks in an acquired diffractogram is proportional to grains in the illuminated volume of the sample. It is therefore expected to be a notable difference in intensity of diffraction peaks among the tempers, where O should yield a higher intensity than the others. Since the granular size is larger in unhomogenised samples, this is expected to show as a higher peak intensity in diffractograms. [16] [17]

2.4 Softening Curve

When a material undergoes cold deformation, the material properties change and the metal hardens. The increased strength is caused by the dislocations and the increase is approximately proportional to the square root of the dislocation density. On the other hand, upon heating the material softens, as a result of recrystallisation. [12]

A softening curve is an analytical method to visualise the changes in material properties upon annealing, as an effect of recrystallisation. To obtain a finished softening curve, the material is cut into different pieces which are annealed at various temperatures. The samples are then placed in a tensile test machine which applies a pulling force to the strips, until breakage. From this yield point, tensile strength, and elongation, generally abbreviated $R_{p0.2}$, R_m, and A_{50mm}, respectively, can be determined. The yield point is defined from the stress-strain curve obtained during the tensile test. If no distinguishable point is present in the curve, an arbitrary

yield point is set, usually at 0.2 % plastic strain. The tensile strength is the obtained maximum of the stress-strain curve and elongation is measured on the sample. Elongation is generally expressed as a percentage of the original sample length. [23] [24]

By presenting the results for a series of temperatures in the same graph it is possible to follow the changes in material properties upon annealing as can be seen in Figure 2.3. Cross sectional pictures of each sample can be acquired using LOM to visually follow the recrystallisation process, since this cannot be done by analysing the softening curves themselves.

At low temperatures a deformed material has a fibrous structure and is therefore very hard. Consequently a high force is needed to reach the yield point and tensile strength of the material. A fibrous structure may also be quite brittle, resulting in a small elongation before fracture of the material occurs. The more recrystallised the material, the softer it will become due to lower strain energy. As a result of this both the yield point and tensile strength will require significantly lower forces to occur while an increase in elongation is obtained. [11] [12]

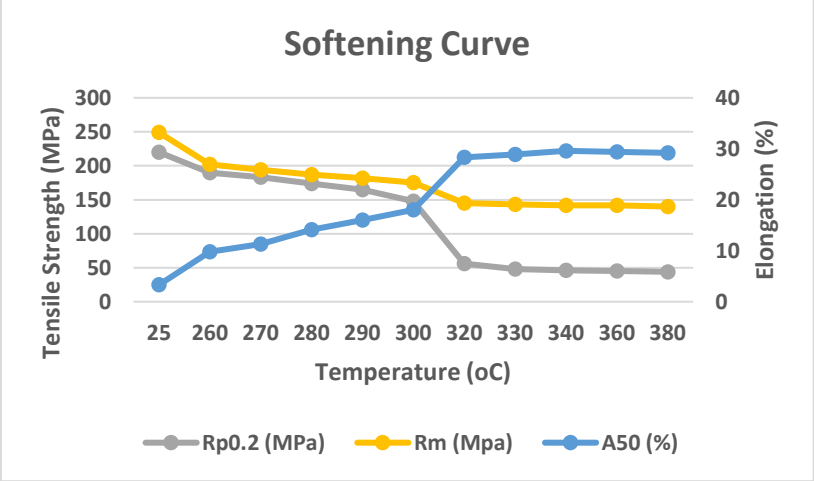

Figure 2.3: Typical example of a softening curve. [24]

In the figure, a change in the parameters is seen when altering the annealing temperature. Although, above 320 ^{o}C no significant change of the parameters is obtained, this since the metal is fully recrystallised. As the material properties change with the degree of recrystallisation, it is expected to see a change in XRD peak intensity even between shorter ranges of temperature.

The series of temperatures used to create the curve is generally determined by the temperature at which the recrystallisation, and therefore change of material properties, occurs. In studies conducted on similar materials [12] [25], the recrystallisation temperature of AA3003 is expected to be close to, but sub, 300 ^{o}C. The closer the temperature intervals, the more precise the visualisation of the change. Normal is to examine the material at every 20th or 10th ^{o}C.

3 Method

Below is described the methodology of the production of the materials used. Further the experiments conducted are presented in detail.

3.1 Sample Fabrication

The alloy used, AA3003, was DC casted to obtain a uniform crystalline structure of the aluminium alloy. After casting, the ingot was either homogenized by heating to 600 ^{o}C, or stored directly. Since the homogenisation was performed on entire ingots, two ingots, one homogenised and one unhomogenised, were used to produce the material used during the experiments. The chemical composition of both ingots was determined during fabrication.

After homogenization, and storage, the material was preheated before hot rolling and later cold rolled to a thickness of 0.8 mm. In this study, the thickness used was 0.3 mm and the material was therefore further cold rolled post production to obtain desired thickness. Four different tempers were used, O, H18, H14, and H24. H18 was obtained by simply cold rolling the material to 0.3 mm while O first was cold rolled to 0.3 mm, to later be fully annealed at 350 ^{o}C. H14 was first cold rolled to 0.46 mm which corresponds to 35 % reduction, annealed at 350 ^{o}C and finally cold rolled to 0.3 mm. H24 was cold rolled directly to 0.3 mm and then tempered at 220 ^{o}C until the correct temper was obtained. During annealing, the temperature was increased by 50 ^{o}C per hour until desired temperature was attained, which was then held for two hours. The temperature was then decreased at the same rate. After this, cross sectional images of all different tempers were acquired using LOM.

3.2 X-Ray Diffraction

The procedures followed when operating the diffractometer for XRD measurements are described below. Two different diffractometers were used in order to performed the experiments. All measurements were performed using a line-focused copper anode source, giving an X-ray wavelength of $\lambda = 0.154$ nm, operated at 45 kV and 40 mA.

3.2.1 Alignment

Before each round of measurements an alignment of the diffractometer was performed to ensure measurements being as accurate as possible. During this procedure the primary and secondary beams were conditioned as described below, in sections 3.2.2 and 3.2.3. An additional Cu filter was used on the secondary beam to reduce the X-ray intensity when measuring the direct beam. A 2θ scan was performed with a step size of 0.2^{o} per step and 2.17 seconds dwell time per step. During annealing experiments the position of the sample holder was aligned before each measurement by performing Z and ω scans. Based on the results obtained, the alignment of the detector was adjusted accordingly.

3.2.2 Room temperature

XRD measurements for each different sample were conducted using a Panalytical X'pert^3 Pro powder diffractometer, with the detector X'Celerator. The primary beam was conditioned by two 1/2^o slits and in the secondary beam a 5 mm slit was placed. The detector was used in scanning line mode for data acquisition. A 2θ-ω scan was performed in a 2θ range of 20^o – 100^o with a step size of 0.02^o and dwell time per step being 50 seconds. Peak correspondence was determined through computer program HighScore, and some calculations according to section 2.1.4. Diffractograms were measured on samples from all four different tempers, and both homogenised and unhomogenised material, adding up to eight different samples.

3.2.3 Stepwise Annealing

For the annealing experiments a Panalytical Empyrean diffractometer was utilised for the measurements, and an Anton-Paar DHS1100 heating stage with a graphite dome was used for the annealing. In the experiments the primary beam of the diffractometer was conditioned by an X-ray mirror, a 1/2^o divergence slit and a 2 mm mask. In the secondary beam a 0.27^o parallel plate collimator was placed. The detector used for data acquisition was a PIXel detector, operated in 0D mode. Each measurement, θ-2θ, was performed in a 2θ range of 42.7^o – 46.7^o, using a step size of 0.03^o and dwell time per step being 1.76 seconds.

During these experiments exclusively samples of homogenised and unhomogenised H18 were used since this temper is the only of the four that has not been treated with heat during the sample preparation. Diffractograms were first acquired at 40 ^{o}C, the temperature were then rapidly increased to desired temperature, at which the sample was annealed for ten minutes, before rapidly decreasing the temperature to 40 ^{o}C, where another diffractogram was acquired. An example of the process can be seen in Figure 3.1. The process was repeated for 220, 240, 260, 270, 280, 290, 295, 300, 320, and 350 ^{o}C for both homogenised and unhomogenised materials, changing the sample before each new cycle.

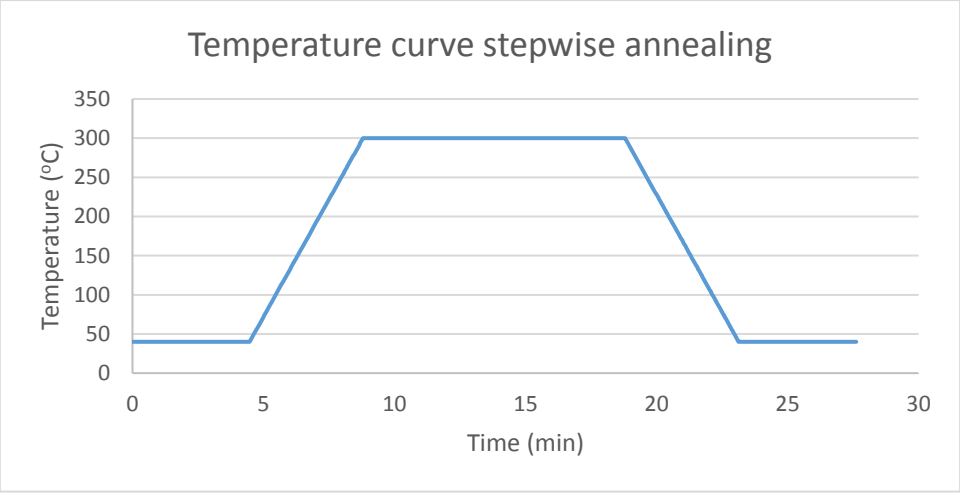

Figure 3.1: Example of the temperature curve used during stepwise annealing, here up to 300 ^{o}C.

3.2.4 Cycled annealing

For the second annealing experiment, the same diffractometer and settings were used as stated in 3.2.3. During these experiments exclusively materials of H18 temper was analysed for the same reason as during stepwise annealing. Here the temperature was cycled according to Figure 3.2. Diffractograms were acquired at room temperature after each annealing cycle, at 40 ºC.

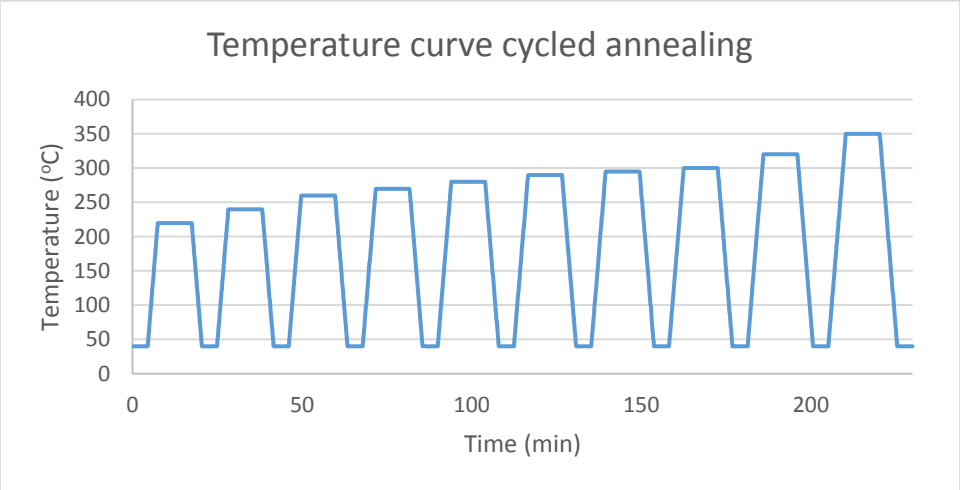

Figure 3.2: Temperature cycles used during annealing experiments.

3.3 Light Optical Microscope

Images of the longitudinal cross section of the samples acquired after fabrication and during the experiments in section 3.2.3 were recorded using LOM.

Before this, the sample pieces were embedded in a block of bakelite. A cut was placed along the rolling direction and the exposed samples were polished in six steps using different abrasives during every step, according to a standard internal method at Gränges, this to ensure a smooth surface. The various specimens are then examined at 50, 100, and 200 times magnification using LOM.

4 Results

Presented below are the results obtained from the experiments conducted during the study.

4.1 Alloy Composition

The results of the chemical analysis are shown in Table 4.1. The composition of each alloying element is within the required intervals, when compared to Table 1.2.

Table 4.1: Chemical analysis of the two ingots used to produce the material.

	Al	Mn	Cu	Fe	Mg	Si	Zn	Res. tot	Res. each
Hom	98.05	1.10	0.12	0.49	0.03	0.13	0.01	< 0.05	< 0.02
Unhom	97.90	1.22	0.12	0.51	0.04	0.11	0.01	< 0.06	< 0.03

4.2 X-Ray Diffraction

To improve readability, results from the different experiments will be separated.

4.2.1 Room Temperature Measurements

The diffractograms of all samples are presented in Figure 4.1 and Figure 4.2, where results from homogenised materials can be seen in the former and unhomogenised in the latter. Note that the different diffractograms are vertically shifted by 50 000 and 100 000 counts for homogenised and unhomogenised samples respectively. Therefore only comparison of peak intensity between the tempers is possible.

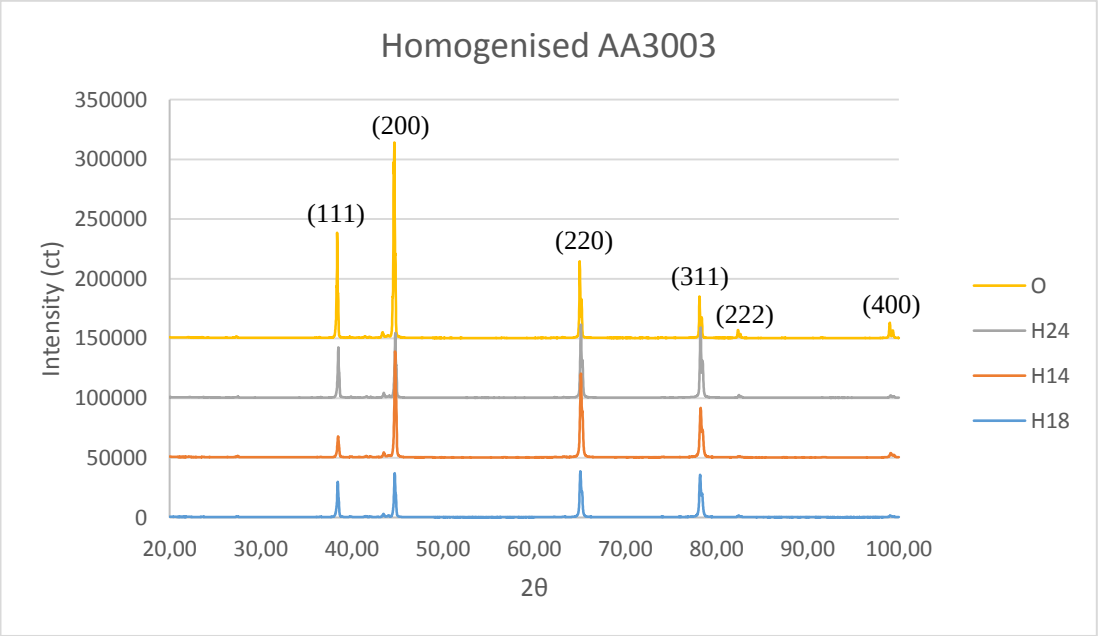

Figure 4.1: Measured diffractogram of homogenised AA3003 at different tempers.

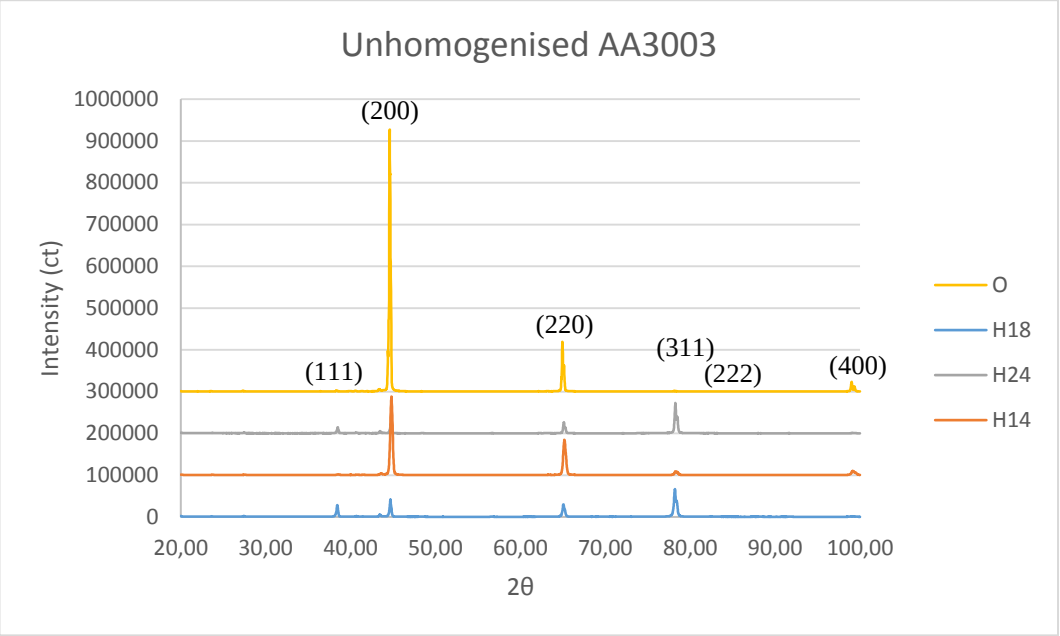

Figure 4.2: Measured diffractogram of unhomogenised AA3003 at different tempers.

The peaks in the above shown diffractograms, Figure 4.1 and Figure 4.2, were identified. Larger peaks, at about 38º, 45º, 65º, 78º, 82º, and 98º, correspond to aluminium planes (111), (200), (220), (311), (222) and (400), as marked in the figures. An overlap of peaks from aluminium blends such as AlSi, AlTi, and AlZn is possible. Not all of the smaller peaks were identified, however some correspond to Fe and Al_6Mn. No peaks of aluminium oxides could be detected.

The largest difference in intensity between the four tempers is seen in peak Al (200), a close-up of this peak can be seen for homogenised and unhomogenised materials in Figure 4.3 and Figure 4.4, respectively.

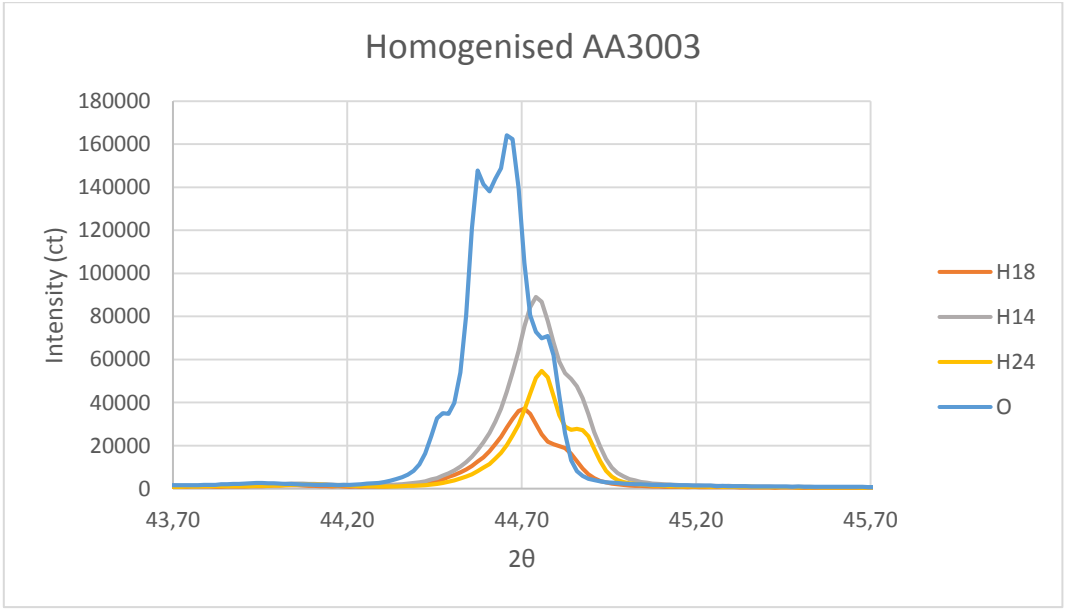

Figure 4.3: Close-up of peak Al (200) in homogenised AA3003.

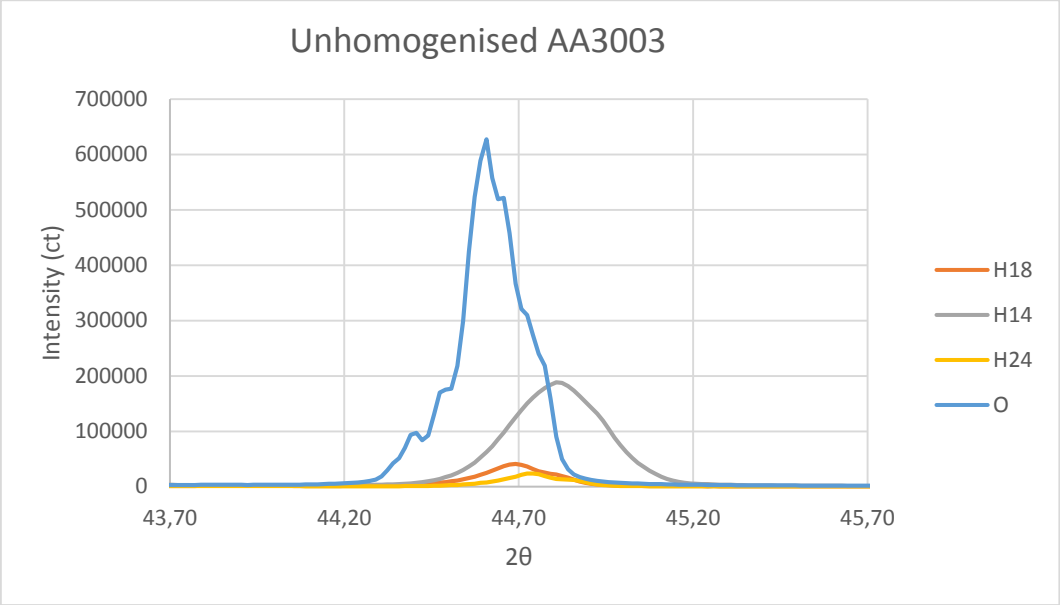

Figure 4.4: Close-up of peak Al (200) in unhomogenised AA3003.

4.2.2 Stepwise Annealing

Diffractograms acquired during stepwise annealing experiments are presented in Figure 4.5 and Figure 4.6. Since all measurements were conducted on different samples, the intensity of the room temperature diffractogram for each specific sample is subtracted from the diffractogram acquired after annealing. This to simplify comparison between the temperatures.

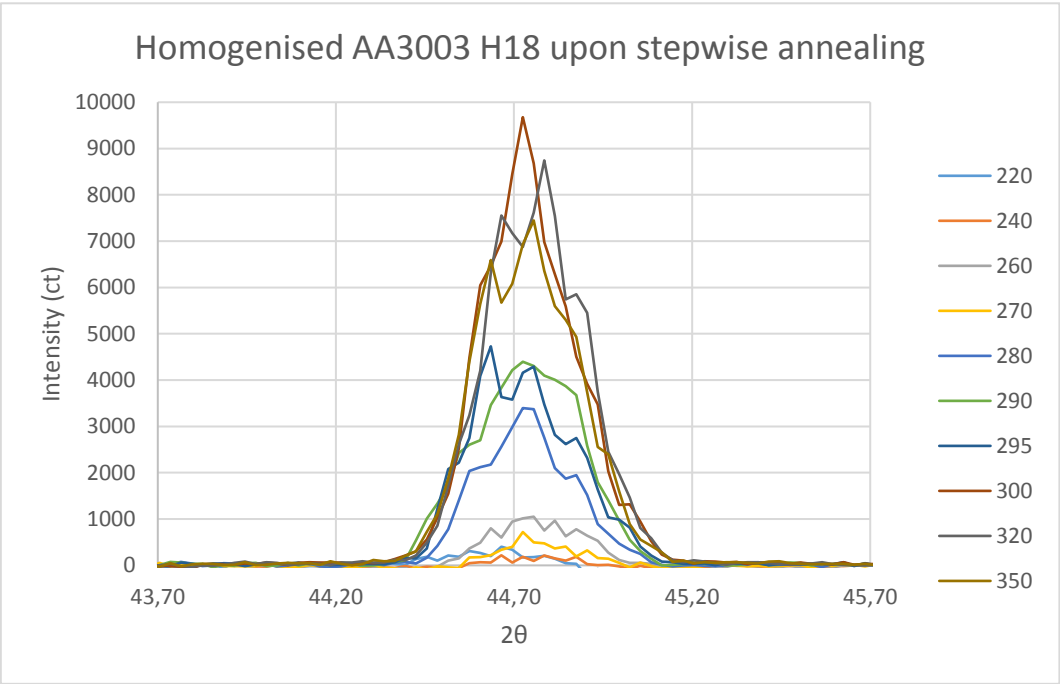

Figure 4.5: Intensity change of Al (200) in homogenised AA3003 H18 upon stepwise annealing.

.

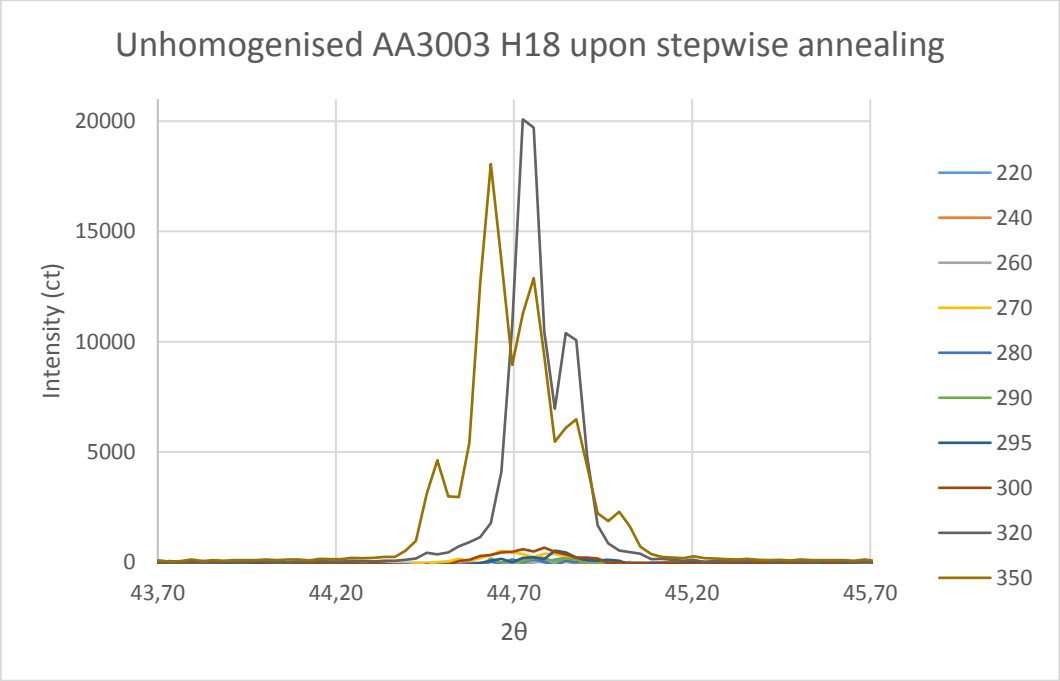

Figure 4.6: Intensity change of Al (200) in unhomogenised AA3003 H18 upon stepwise annealing.

4.2.3 Cycled Annealing

Results from the cycled annealing experiments are presented in Figure 4.7 and Figure 4.8 below.

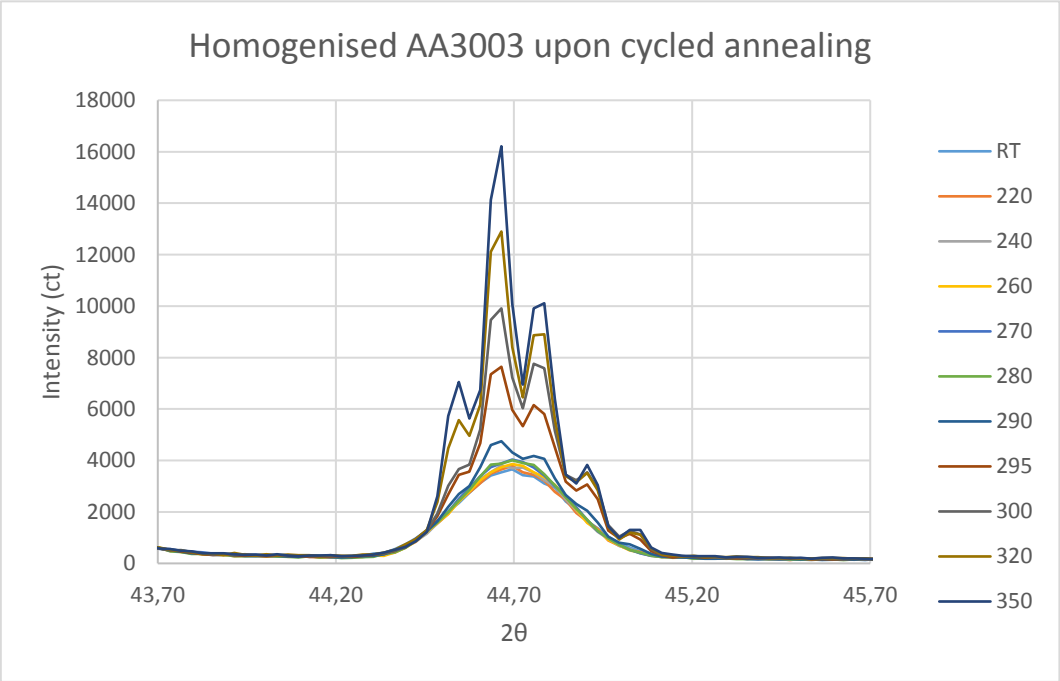

Figure 4.7: Intensity of Al (200) in homogenised AA3003 H18 during cycled annealing.

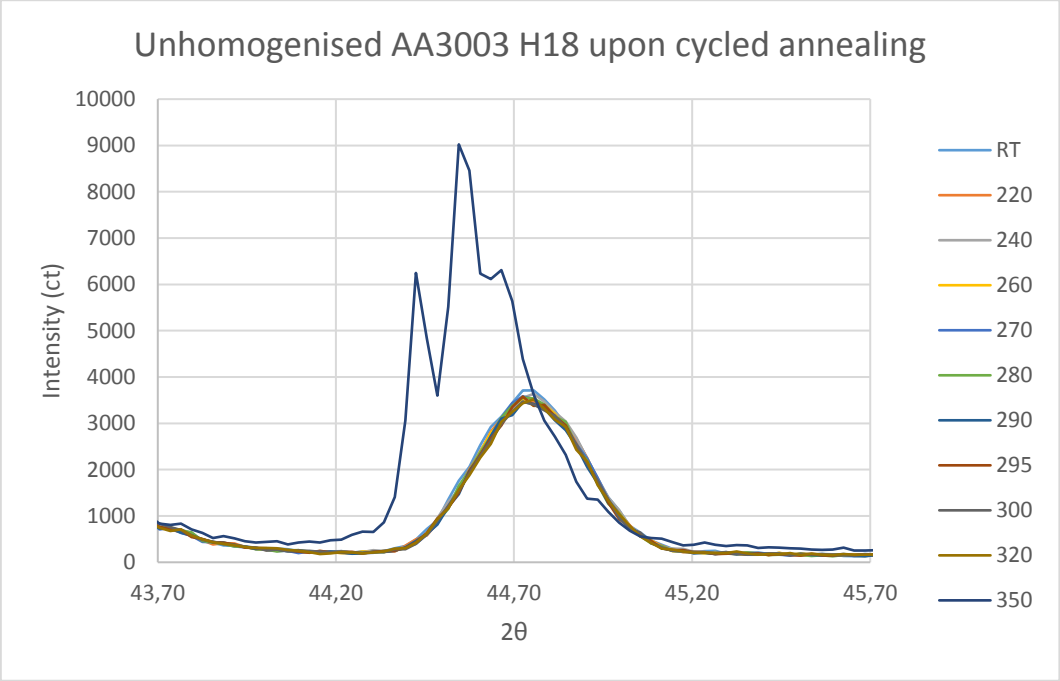

Figure 4.8: Intensity of Al (200) in unhomogenised AA3003 H18 during cycled annealing.

4.3 Change in Crystallite Size

In Figure 4.9 the change in the aluminium (200) peak maximum intensity is presented, to simplify comparison between the experiments.

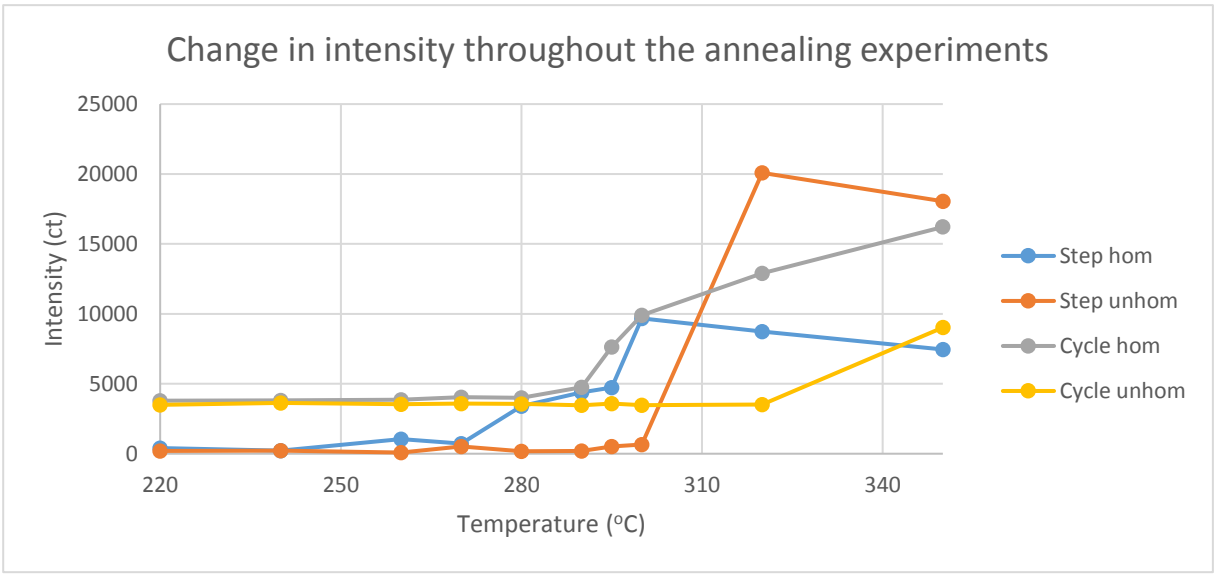

Figure 4.9: Peak maximum at different temperatures for the annealing experiments.

Figure 4.10 shows the intensity change in the integrated intensity of the aluminium (200) peak in diffractograms from the stepwise and cycled annealing experiments.

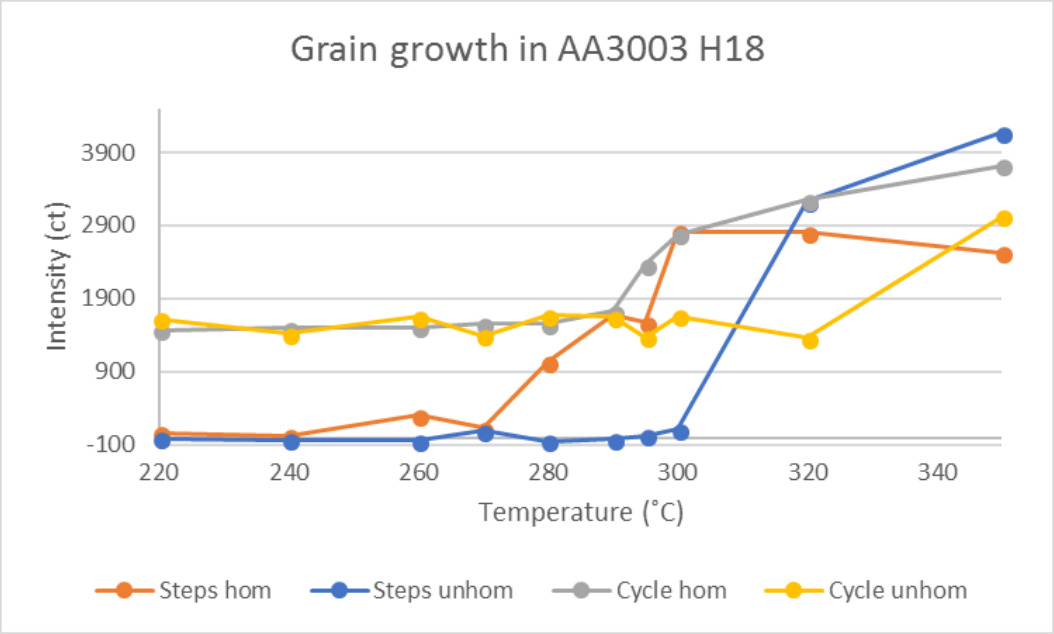

Figure 4.10: Summarised intensity beneath Al (200) at different temperatures.

4.4 Grain Structure

Images of all samples created during stepwise annealing were acquired using LOM. Homogenised samples are presented in Figure 4.11 and unhomogenised in Figure 4.12 below. All images are denoted with the temperature, in °C, at which the annealing was conducted.

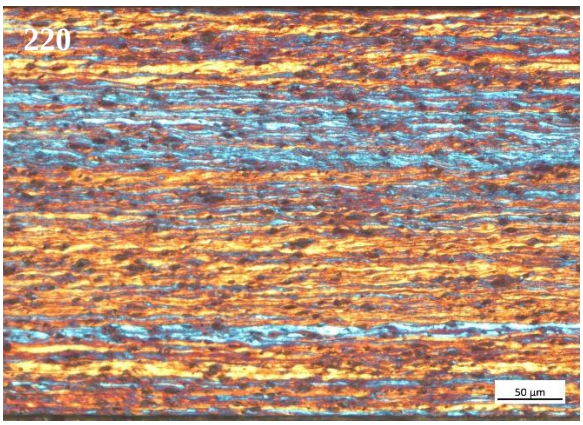

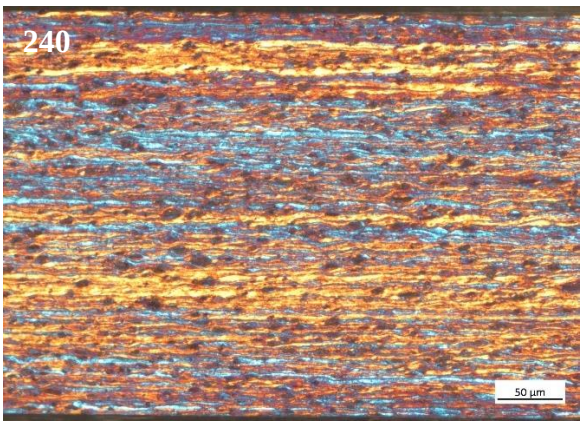

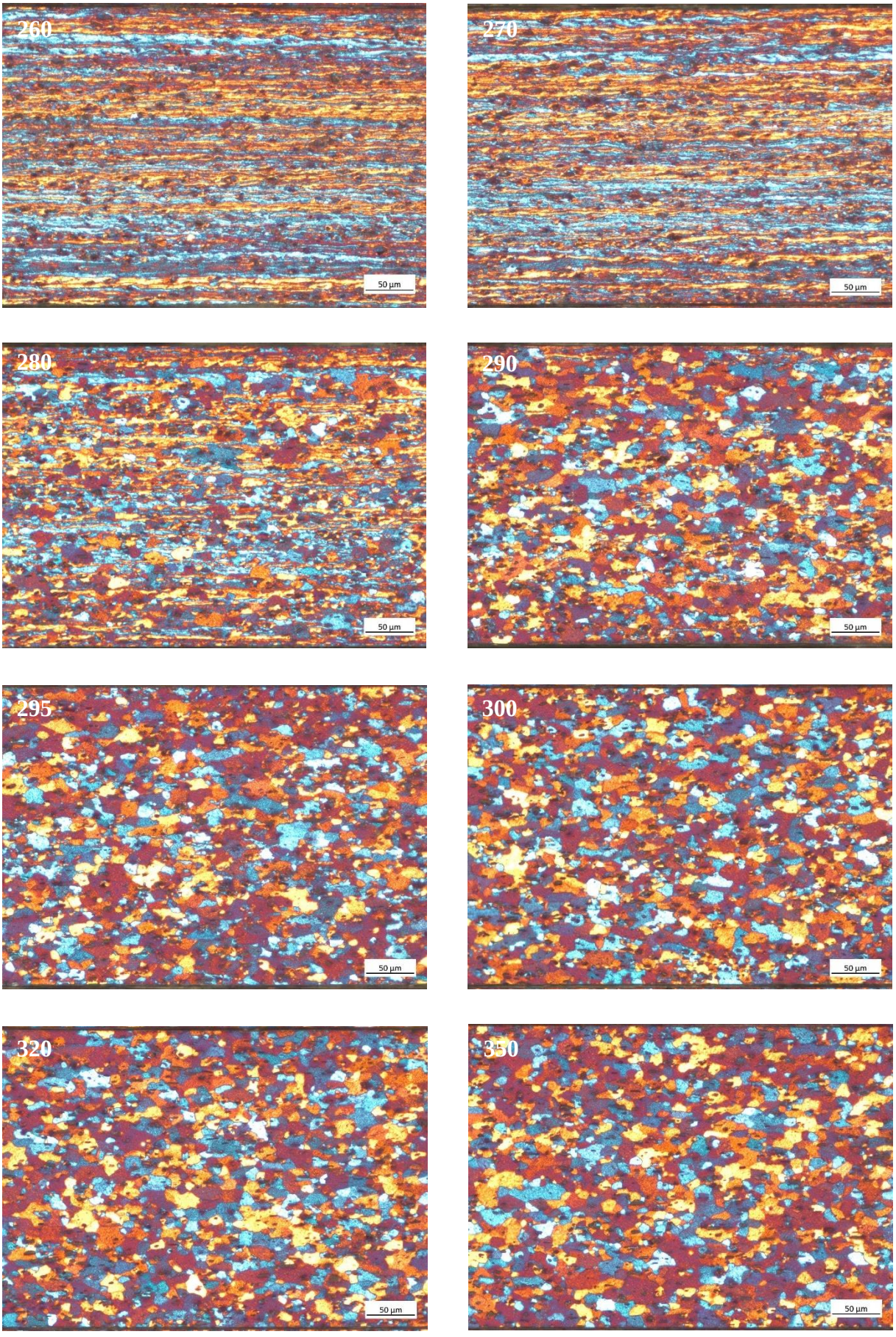

Figure 4.11: Longitudinal images of cross section of homogenised samples.


220
50 µm

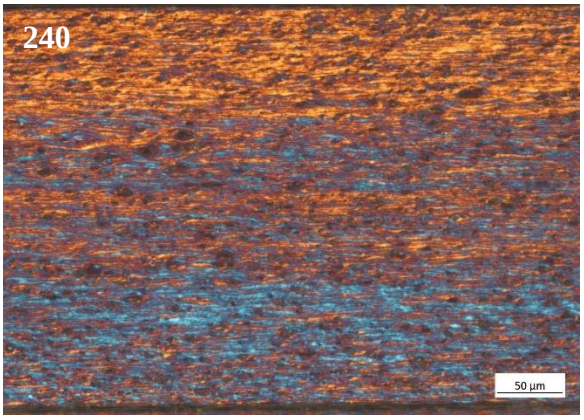
240
50 µm


260
50 µm

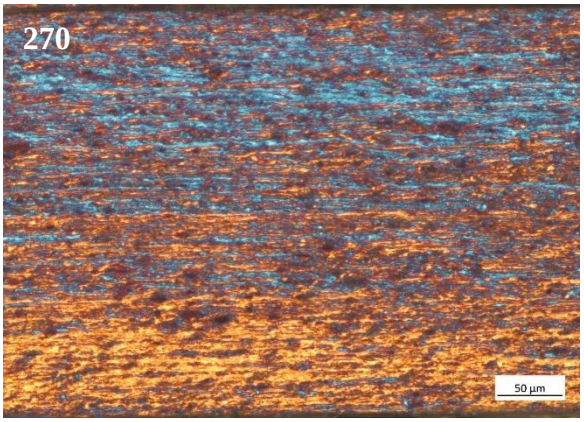
270
50 µm

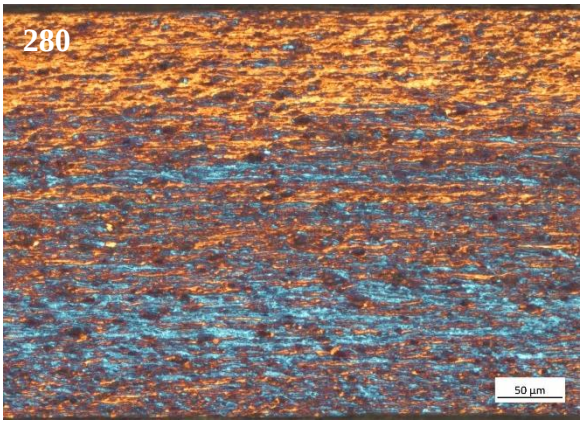
280
50 µm

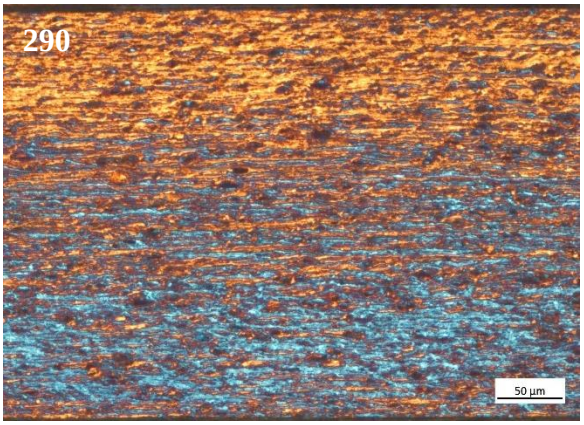
290
50 µm

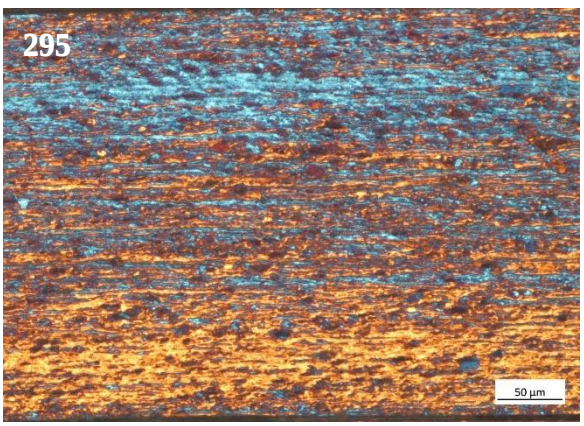
295
50 µm

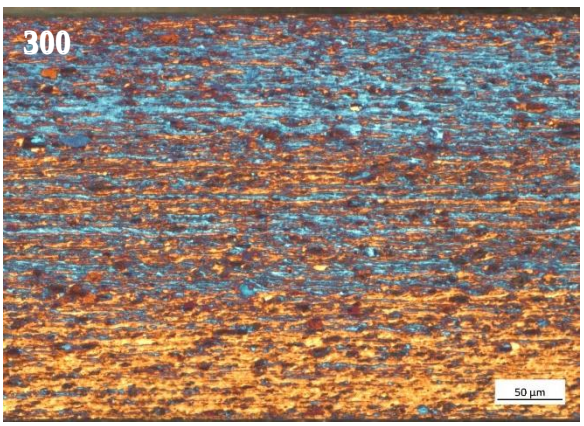
300
50 µm

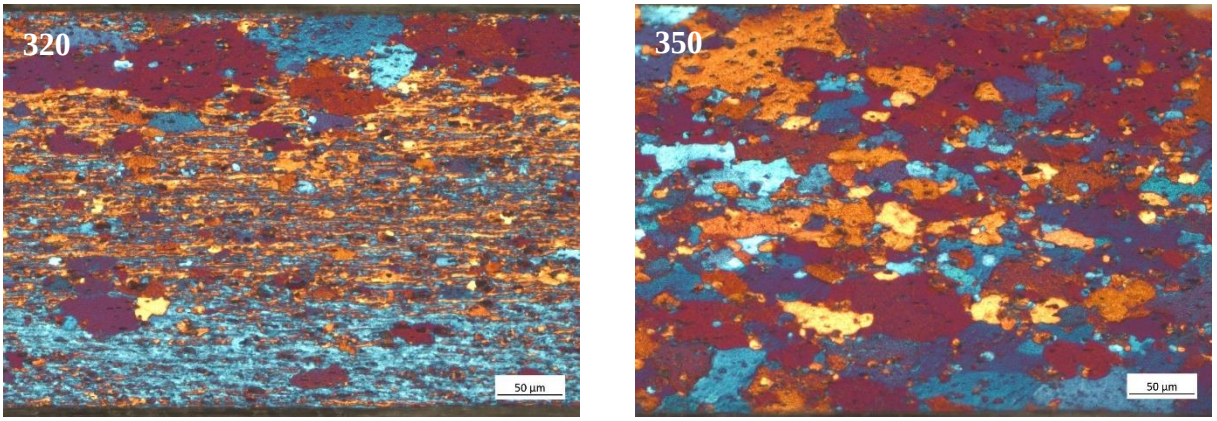

Figure 4.12: Longitudinal images of cross section of unhomogenised samples.

5 Analysis and Discussion

In the following chapter the different major parts of the study will be discussed, starting with the analysis of the results obtained, discussion about the method used, and finally some notes about possible future work.

5.1 Results

In the close-up of the Al (200) peak in Figure 4.3 and Figure 4.4, a slight shift towards lower angles of the peak for O temper may be noted. This is thought to be due to a thermal expansion of the material upon annealing. Expansion of the material will lead to an increase in interplanar spacing of the material, hence a shift towards smaller diffraction angles in the diffractogram will appear according to Bragg's law. This may complicate the analysis of the peak correspondence, however since the composition of the material is know the incorrect peak calculations can be accounted for. Thus this matter will not be further discussed here. As seen in Figure 4.1 and Figure 4.2, the largest difference in peak intensity between the tempers lies in peak Al [200]. The reason for this is probably due to texture in the material as a result of cold deformation during the fabrication process.

When comparing Figure 4.1 and Figure 4.2, the latter graph shows significantly higher intensities for most peaks. This is due to the fact that during homogenisation the crystallite sizes become more uniform and usually smaller than right after casting. The larger grains of unhomogenised material lead to an increase of some grain orientations in the illuminated area and thus higher intensities for said peaks. Further, almost no peaks, apart from aluminium, is visible in the diffractogram of unhomogenised materials. In Figure 4.1, homogenised material, some smaller peaks corresponding to Al_6Mn can be seen at lower angles.

In the results from the annealing experiments performed, Figure 4.5 – Figure 4.8, a distinct change in peak intensity upon annealing is visible. Between the stepwise and cycled annealing the results are similar to the eye, however the difference between homogenised and unhomogenised H18 is striking. For the homogenised samples a change in peak intensity occur at approximately 280 ^{o}C, while there is no significant change in intensity until, at least, 300 ^{o}C for the unhomogenised samples. This is believed to occur because the unhomogenised samples contain larger grains to begin with, and therefore has a lower free energy from grain boundaries and dislocations in the bulk material. This would in turn affect the recrystallisation process and more external energy is needed for initiation. In said figures, the peaks appear to be split into several thinner peaks. This phenomenon is thought to be due to an artefact from the equipment used.

In Figure 4.9 it can be seen that the change in peak intensity occur slightly later during cycled annealing experiments than if the samples were exchanged between each annealing cycle. This shift probably occurs since recovery of the material takes place during earlier temperature cycles and therefore the free energy of the material is slightly lowered and the

recrystallisation process is therefore delayed into higher temperature cycles. Thus, cycled annealing might not reflect the true behaviour of the examined metal.

The longitudinal cross section images of homogenised samples in Figure 4.11 show no noticeable recrystallisation until 280 ^{o}C, where formation of new grains can be distinguished. At 295 ^{o}C the metal appear to be fully recrystallised, and no significant grain growth can be distinguished with increasing temperature. This is thought to be caused by the heavily texture of the material and therefore the driving force for grain growth is inhibited. The unhomogenised counterpart, Figure 4.12, shows no recrystallisation until 300 ^{o}C where tendencies to grain formation is visible and the metal seems to be fully recrystallised at 350 ^{o}C. Even here it is clear that the size of the recrystallised grains are markedly larger when comparing the homogenised and unhomogenised materials in the two figures.

When comparing Figure 4.11 and Figure 4.12 to Figure 4.9 it seems like the observed change in peak intensity quite nicely corresponds to the degree of recrystallisation seen in the cross sectional images. Figure 4.10 show almost identical results as Figure 4.9, the difference being an increase in intensity between 320 and 350 ^{o}C for the unhomogenised sample during cycled annealing. This could indicate grain growth, a theory that is confirmed by the images shown in Figure 4.12. Based on above stated reasons, it is safe to assume that the recrystallisation process can be characterized using *in situ* heating during XRD measurements.

5.1.1 Sources of Error

The samples used during XRD measurements were simply cut from metal sheets using scissors, resulting in the samples to be slightly dented, especially around the edges. Since attempts were made to correct the problem, and measurements were conducted using a so called parallel beam geometry the problems with shifted peaks should be accounted for. Considering the peaks of aluminium being situated approximately the same positions for each measurement, this can be confirmed.

Further, the dents on the samples could have affected the heat distribution to the material during annealing. This since the oven, the Anton-Paar DHS1100, used for heating consists of a heating plate, onto which the sample pieces were placed. Therefore, if the sample had been a subject for extensive denting the annealing could have been partial or unevenly distributed in the metal.

Furthermore, the oven used during the *in situ* XRD could not be calibrated and therefore the temperature shown on the display may not entirely correspond to the true temperature. Therefore, the actual temperature might have differed from the desired. However, the displayed temperature difference does correspond well to the true temperature difference.

5.2 Method

Since no earlier studies conducting the same investigations were found, the stepwise annealing experiments are mainly based on customary procedures at Gränges and the cycled annealing on a combination of several different methods found in articles during the literature study. Usually, the recrystallisation process, from different points of view, is the main subject studied, although during this thesis work the goal was to evaluate characterisation of recrystallisation using *in situ* XRD during heating. The cycled annealing experiments were developed as a more time and resource efficient alternative to the stepwise annealing.

5.2.1 Source Criticism

During the literature study, presented in Chapters 1 and 2, mainly scientific articles were used to gather the information needed to obtain sufficiently profound knowledge of the field and previous work. Provided by Gränges were numerous printed sources, which were used to gain a basic understanding about aluminium, its alloys and the characterisation methods utilised. The chemical composition of alloy AA3003 could not be found in published scientific articles and is therefore retrieved from the website of Atlas Steel, a retailer of the alloy. This information is considered to be commonly known, and have been compared to several different sources, and it is therefore safe to assume that Atlas Steel presents the correct composition. Further, the source of information to the written chapter about the company, section 1.3.1, is Gränges' own website and is therefore considered to be a reliable source.

5.2.2 Project oversights

In the scope of this thesis work, only the change of one chosen peak was analysed. The reason for this was to simplify the analysis and to save time. However, analysing the entire range on the diffractogram, or at least a handful of peaks, might have shown different or more conclusive results.

Customary in industry is heating the samples slowly, about 50 ^{o}C per hour, when annealing. During the annealing experiments the heating rate was kept much higher, at 60 ^{o}C per minute, due to the time constraints and equipment limitations. As described in section 1.3.3.4, the heating rate can have an impact on the recrystallisation temperature, this has consequently not been taken into consideration when conducting the experiments. However, when looking to other experiments conducted by H.-E. Ekström [12] this effect does not seem to have affected the results.

5.3 Future work

Recrystallisation of metals have a great impact on the material properties and thus, the area of use can be altered depending on the process. If the recrystallisation can be modified as desired it will be possible to obtain stronger materials and thus, construct lighter structures for example the car industries. Since only one aluminium alloy was studied during the experiments conducted, to proceed, other alloys and metals should be investigated using the

same method. Should it turn out to be possible to obtain the same information from using other materials, further investigations of recrystallisation and improvement of method efficiency could be next.

Furthermore, based on results obtained from an *in situ* heat treatment measurement, a relation between degree of recrystallisation and temperature may be demonstrated. Based on this, it is possible to choose an optimal temperature where recrystallisation of the studied material occurs at sufficiently low rate. By performing measurements at different temperatures the activation energy of the recrystallisation process is presumably possible to determine. This, if it is possible to implement, it would not only be a great knowledge, but also open up a new door in fine tuning properties of materials for different applications.

More interesting studies could be conducted using a diffractogram which can perform measurements for a shorter period of time and with a higher accuracy. This could be done using, for example, a synchrotron radiation facility, in which *in situ* annealing can be conducted simultaneously with acquiring diffractograms. Thus, allowing closer to real time measurements of the recrystallisation process. This would eliminate estimations made executing stated experiments and therefore improving the resulting conclusions, thus yielding a greater understanding of the subject.

6 Conclusions

During this thesis work it has been studied whether it is possible to characterise the recrystallisation process of aluminium alloy AA3003 using *in situ* XRD during heating. From the results obtained, the conclusion can be drawn that it in fact is possible to do this. A clear change in intensity of peaks in the diffractogram, that follows the recrystallisation visualised using LOM, can be seen. Due to some sources of error and the inability to obtain cross sectional images from the cycled annealing experiments, the method is considered inferior to stepwise annealing.

Stepwise annealing show potential and it is therefore encouraged to further investigate the method in order to improve the working procedures as well as extending the materials used. The method is considered a good complement to the traditional softening curves, since an estimate of crystallite size can be obtained. Furthermore, by using diffractometers with superior acquisition time to the ones used during this work the recrystallisation could be investigated in real time and the knowledge of recrystallisation could be further increased.

7 References

[1] Gränges Innovative Aluminium Engineering, “About Gränges,” Gränges, 2018. [Online]. Available: http://www.granges.com/about-granges/. [Accessed 15 Februari 2018].

[2] Gränges Innovative Aluminium Engineering, “Gränges Innovative Aluminium Engineering,” Gränges, 2018. [Online]. Available: http://www.granges.com/. [Accessed 02 Februari 2018].

[3] Gränges, “Effektiv och avancerad tillverkning i alla Gränges regioner,” Gränges Innovative Aluminium Engineering, 2018. [Online]. Available: www.granges.com/sv/om-granges/var-verksamhet/produktionsanlaggningar. [Accessed 24 March 2018].

[4] B. Thundal, Aluminium, Kristianstad: Almqvist & Wiksell Förlag, 1991.

[5] C. Nordling and J. Österman, Physics Handbook for Science and Engineering, Lund: Studentlitteratur, 2006.

[6] C. Vargel, Corrosion of Aluminium, Kidlington, Oxford: Elsevier Ldt, 2004.

[7] K. Ahlberg, Materiallära Modul 6.2 B1 Aluimnium, Ljungbyhed: Flygteknikcenter, 2013.

[8] F. Humphreys and M. Hatherly, Recrystallization and Related Annealing Phenomena, 2 ed., Kidlington, Oxford: Elsevier Ldt, 2004.

[9] S. Suwas och R. K. Ray, Crystallographic Texture of Materials, London: Springer, 2014.

[10] Atlas Steels, “Atlas Steels Aluminium Alloy Data Sheet 3003,” October 2013. [Online]. Available: http://www.atlassteels.com.au/documents/Atlas_Aluminium_datasheet_3003_rev_Oct_2013.pdf. [Accessed 18 May 2018].

[11] D. A. Porter, K. E. Easterling and M. Y. Sherif, Phase Transformations in Metals and Alloys, 3 ed., Boca Raton: Taylor & Francis Group, 2009.

[12] H.-E. Ekström, “The softening mechanisms during annealing of cold rolled Al-Mn alloys,” Sapa Technology, Finspång, 2010.

[13] G. T. Barnes and I. R. Gentle, Interfacial Science: An Introduction, 2 ed., New York: Oxford University Press, 2011.

[14] D. Santu, N. Gayathri, M. Bhattacharya and P. Mukherjee, “In Situ XRD Studies of the Process Dynamics During Annealing in Cold-Rolled Copper,” *Metallurgical and Materials Transactions A,* vol. 47, no. 12, pp. 6281-6291, 2016.

[15] J.-H. Cho, H.-P. Ha and K. Oh, “Recrystallization and Grain Growth of Cold-Rolled Gold Sheet,” *Metallurgical and Materials Transactions A,* vol. 36, no. 12, pp. 3415-3425, 2005.

[16] S. Poulsen, E. Lauridsen, A. Lyckegaard, J. Oddershede, C. Gundlach, C. Curf and D. Juul Jensen, “In situ measurements of growth rates and grain-averaged activation energies of individual grains during recrystallization of 50% cold-rolled aluminium,” *Scripta Materialia,* vol. 64, pp. 1003-1006, 2011.

[17] L. Hashemi-Sadraei, S. E. Mousavi, E. J. Lavernia and J. M. Schoenung, “The Influence of Grain Size Determination Method on Grain Growth Kinetics Analysis,” *Advanced Engineering Materials,* vol. 17, no. 11, pp. 1598-1607, 2015.

[18] M. Kühbach, T. Brüggemann, K. Molodov and G. Gottstein, “On a Fast and Accurate In Situ Measuring Strategy for Recrystallization Kinetics and Its Applications on an Al-Fe-Si Alloy.,” *Metallurgical & Materials Transactions,* vol. 46, no. 3, pp. 1337-1348, 2015.

[19] M. Birkholz, Thin Film Analysis by X-Ray Scattering, Weinheim: Wiley-VCH Verlag GmbH & Co, 2006.

[20] M. Etter och R. E. Dinnebier, ”A Century of Powder Diffraction: a Brief History,” *Z. Anorg. Allg. Chem.,* p. 3015, 3 December 2014.

[21] J. Walker, Principle of Physics, 9th ed., Hoboken: John Wiley & Sons, 2011.

[22] S. Amelinckx, R. Gevers, G. Remaut och J. Van Landuyt, Modern Diffraction and Imaging Techniques in Material Science, Amsterdam: North-Holland Publishing Company, 1970.

[23] D. R. Askeland, P. P. Fulay and W. J. Wright, The Science and Engineering of Materials, Boston: Cengage Learning Inc., 2010.

[24] K. Börjesgård, “Softening curve - 8U11 to Valeo,” Gränges Sweden AB, Finspång, 2017.

[25] H.-E. Ekström, ”Mechanical properties of thin strip of AA3103-H19,” Gränges Technology, Finspång, 1998.